International Journal of Nanoelectronics and Materials
IJNeaM
ISSN 198-5761 | E-ISSN 2232-1535

Effect of Multiple Reflow Cycles and Isothermal Aging on Shear Strength in SAC305/Sn58Bi/Cu-OSP Hybrid Solder Joint

Muhammad Luqman Mokhtar[a,b], Flora Somidin[a,b,*] and Mohd Arif Anuar Mohd Salleh[a,b]

[a]*Electronic Packaging and Thin Film Materials, Centre of Excellence Geopolymer & Green Technology (CeGeoGTech), Universiti Malaysia Perlis (UniMAP), Taman Muhibbah, 02600 Jejawi, Arau, Perlis, Malaysia*
[b]*Faculty of Chemical Engineering and Technology, Universiti Malaysia Perlis (UniMAP), Taman Muhibbah, 02600 Jejawi, Arau, Perlis, Malaysia*
**Corresponding author. Tel.: +60-49798751; e-mail: flora@unimap.edu.my*

ABSTRACT

This study investigates the effects of multiple reflow cycles and isothermal aging on the shear strength and microstructure of SAC305/Sn58Bi/Cu-OSP hybrid solder joints. The joints combine SAC305 solder spheres and Sn58Bi solder paste reflowed on Cu-OSP substrates. Microstructural analysis revealed two distinct regions: a Bi-rich phase at the bottom and an Ag-rich phase at the top. Reflow cycles and isothermal aging at 85 °C, 125 °C, and 150 °C for up to 120 hours were evaluated for their impact on mechanical performance and reliability. Shear tests at 100 mm/s and 2000 mm/s showed that hybrid joints outperformed conventional SAC305/Cu-OSP joints, even after multiple reflow cycles. Aging at 85 °C and 125 °C had minimal impact on shear strength, indicating good stability under moderate conditions. However, aging at 150 °C, above the melting point of Sn58Bi (138 °C), caused a significant decrease in strength. These findings highlight the potential of hybrid solder joints for improved mechanical performance and thermal stability, offering advantages over conventional solder joints for advanced electronic packaging.

Keywords: *SAC305/Sn58Bi, Hybrid solder joint, Cu-OSP, Isothermal aging, Thermal cycling, Mechanical properties*

1. INTRODUCTION

Recent advancements in semiconductor technology have pushed Moore's Law to its limits, driving the adoption of 3D integrated circuits (ICs) with through-silicon vias (TSVs) and vertical stacking. This, along with the rising demand for advanced packaging technologies like Package-on-Package (PoP), has led to the development of hybrid or composite solder joints to improve packaging and joint reliability [1-8].

There is growing interest in hybrid solder joints that combine low-temperature and high-temperature solder alloys, with Sn58Bi, a lead-free solder with a low melting point of about 138 °C. However, studies have shown that the Bi phase is brittle, lacks ductility, and has a low melting point [9-10]. To address these challenges, researchers have recently proposed a mixed solder of SnAgCu/SnBi [2, 3, 4, 11], combining the advantages of both materials. Additionally, Sn3.0Ag0.5Cu (SAC305) solder, commonly used in Ball Grid Array (BGA) packages for its excellent mechanical properties, solderability, and moderate melting point (217 °C), has largely replaced lead-based solders due to compliance with the Restriction of Hazardous Substances (RoHS) directive.

While hybrid soldering, which blends high-temperature solders like SAC305 with low-temperature solders like Sn58Bi, offers the advantage of optimizing the strengths of both materials, it faces challenges during repeated reflow cycles and prolonged isothermal aging, typical in multi-pass soldering processes [12-14]. Repeated thermal cycling can induce microstructural changes that degrade the mechanical properties of solder joints, while isothermal aging alters microstructural characteristics, often leading to reduced shear strength and joint reliability.

This study aims to investigate the effects of multiple reflow cycles and isothermal aging on the microstructural evolution and mechanical properties of SAC305/Sn58Bi/Cu-OSP hybrid solder joints. Through a detailed analysis of shear strength under varying thermal and aging conditions, this research seeks to provide valuable insights into the mechanical performance of hybrid joints, contributing to the optimization of low-temperature hybrid soldering solutions for more reliable and energy-efficient electronic packaging.

2. MATERIALS AND METHODS

Hybrid solder joints were prepared by assembling SAC305 (Sn3.0Ag0.5Cu in weight percent, wt.%) solder spheres of about 900 µm diameter, Sn58Bi (in wt.%) solder paste, and a Cu-OSP (organic solderability preservative) surface-finished metal substrate with a 900 µm pitch size, as shown in Figure 1(a). The SAC305 solder spheres had a diameter of approximately 900 µm, and the Sn58Bi solder paste was evenly spread on the Cu-OSP substrate using a stencil with apertures and a thickness of approximately

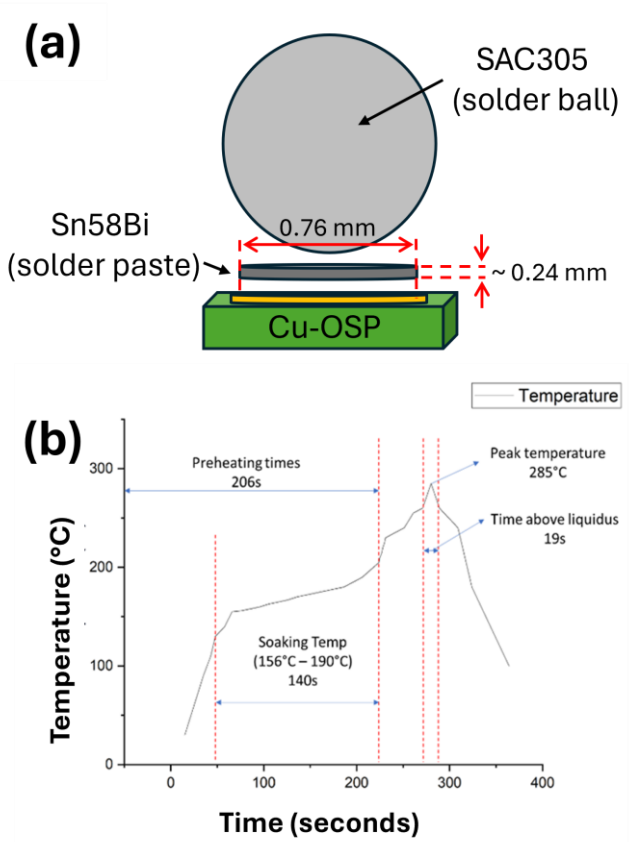

Figure 1. (a) Schematic diagram of the hybrid solder joint arrangement, and (b) temperature profile used for the reflow soldering.

0.76 mm and 0.24 mm, respectively. The solder/substrate samples underwent multiple reflow cycles following the temperature profile shown in Figure 1(b). In this study, the reflow temperature profile was set to accommodate the lead-free SAC305 solder alloy (melting point, Tm = 217 °C) for conventional and hybrid solder joints. Typically, the maximum reflow temperature is set at approximately 30 °C above the solder's melting point to ensure proper soldering. Due to the low thermal conductivity distribution of the reflow oven used in this study; the maximum temperature was set at 285 °C.

The solder joints were then isothermally aged at temperatures of 85 °C, 125 °C, and 150 °C in a furnace for up to 5 days (120 hours). For comparison, conventional SAC305/Cu-OSP solder joints were fabricated using a similar process as a control. To examine the cross-sectional microstructures of the hybrid solder joints, the samples were cold-mounted in epoxy resin, ground with a series of silicon carbide (SiC) papers, and carefully polished using fine alumina particle solutions. Microstructural analysis was performed using a FESEM FEI Nova Nano SEM 450 equipped with energy-dispersive X-ray spectroscopy (EDX) at an accelerating voltage of 10 kV. The impact shear strength of the solder joints was performed with a 50 N shear load at shear speeds of 100 mm/s and 2000 mm/s using a DAGE-4000HS-FD bond micro-tester (Nordson, USA). The shear height was set to 90 µm above the substrate. At least four solder joints were tested for each condition.

3. RESULTS AND DISCUSSION

3.1. Microstructural Observation of The As-Soldered Solder Joints

Figure 2 presents the microstructure of the conventional SAC305/Cu-OSP solder joint following a single reflow cycle. The SAC305 alloy is known to form a Cu_6Sn_5 intermetallic compound (IMC) at the interface with the Cu substrate. It is well established that Ag does not react with Cu and instead forms the Ag_3Sn phase, which is dispersed throughout the Sn matrix in the SAC305 solder bulk [15-16]. The elemental distribution of Ag is particularly prominent in the solder bulk area, as shown in the EDX results in

Figure 2(c-f).

Figure 3 presents the microstructure of the as-reflowed SAC305/Sn58Bi/Cu-OSP hybrid solder joint. The Sn58Bi solder exhibits a characteristic laminar structure composed of white Bi-rich regions and gray β-Sn phases. This performance enhancement in hybrid joints can be attributed to their distinct microstructures, characterized by two alloy layers (

Figure 3). In hybrid solder joints, the Sn-Bi alloy microstructure dominates near the solder/substrate interface, while in conventional SAC305/Cu-OSP joints, only the Sn-Ag-Cu alloy microstructure is present in both

the bulk and solder/substrate areas. Several studies have reported that incorporating a small amount of Bi refines the microstructure, lowers the melting temperature, and improves the mechanical performance of SAC305/Cu solder joints [22-24]. These factors likely contribute to the enhanced shear strength observed in SAC305/ Sn58Bi/Cu-OSP hybrid solder joints.

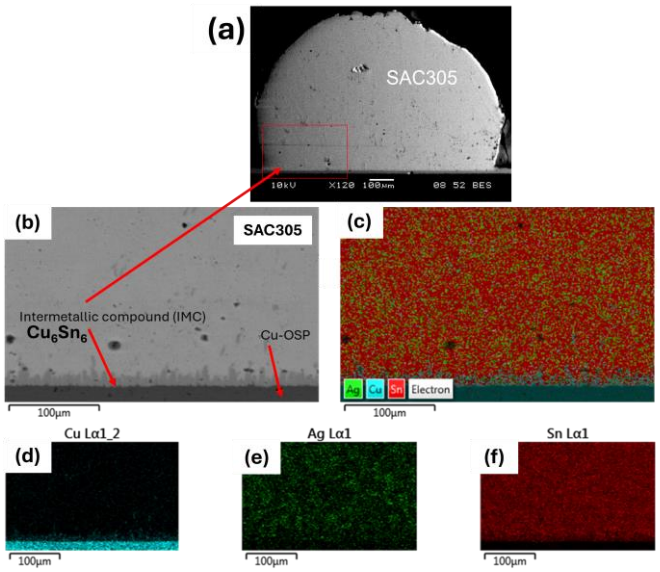

Figure 2 (a-b) Backscattered electron (BSE) SEM images of as-soldered SAC305/Cu-OSP solder joint cross-section. (c) EDX elemental mapping results corresponding to image (b), showing the distribution of (d) Cu elements, (e) Ag elements, and (f) Sn elements.

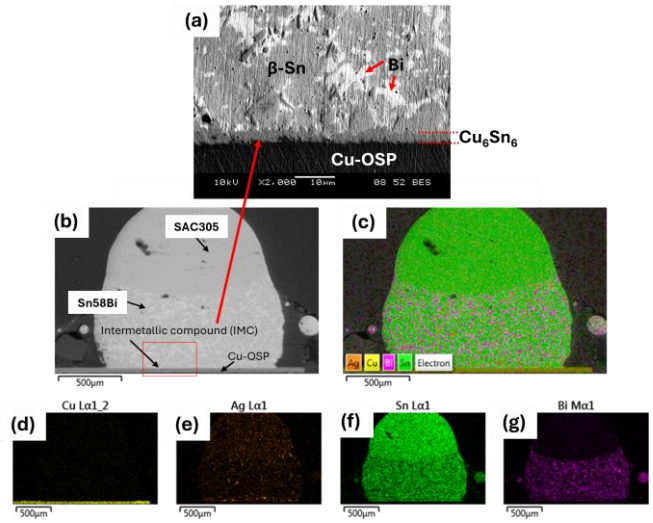

Figure 3. (a-b) BSE-SEM images and (c) EDX elemental mapping of the as-reflowed SAC305/Sn58Bi/Cu-OSP hybrid solder joint. The element mapping of (d) Cu elements, (e) Ag elements, (f) Sn elements, and (g) Bi elements.

Within the SAC305/Sn58Bi/Cu-OSP hybrid solder joint, two distinct regions are evident: a Bi-rich phase concentrated at the bottom and an Ag-rich phase distributed throughout the solder bulk, predominantly concentrated at the top, as shown in the elemental mapping in

Figure 3(c-g). The Cu_6Sn_5 phase serves as the interfacial IMC in Sn-Bi alloy/Cu solder joint [9, 17], as Bi is known not to react with Cu to form an IMC layer. Research indicates that while Bi does not form an IMC with Cu, its segregation can affect the overall microstructure and performance of solder joints. The study by Ren and Collins [18] demonstrates that incorporating Bi alongside Ag enhances the mechanical performance of solder joints while improving their overall reliability during thermal cycling.

3.2. Solder Joint Impact Shear Strength Performance

Figure 4 illustrate the schematic diagram of the ball shear test, emphasizing the fracture areas observed at shear speeds of 100 mm/s and 2000 mm/s, as reported in multiple studies [19-21].

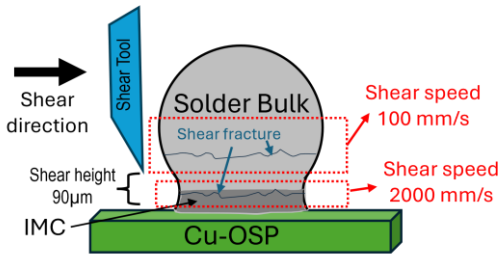

Figure 4. Schematic diagram illustrating the tendency of fracture areas corresponding to shear speeds of 100 mm/s and 2000 mm/s.

At lower speeds, such as 100 mm/s, cracks predominantly propagate through the solder ball, reflecting the mechanical properties of the bulk solder. Conversely, at a shear speed of 2000 mm/s, cracks often extend partially or entirely through the solder/substrate interface, particularly near the intermetallic compounds, emphasizing the strength of this region.

Figure 5 shows the average shear force as a function of reflow cycles for SAC305/Cu-OSP and SAC305/Sn58Bi/Cu-OSP solder joints at low and high shear speeds. Notably, the SAC305/Sn58Bi/Cu-OSP hybrid solder joints consistently demonstrate superior shear strength compared to the conventional SAC305/Cu-OSP joints. For as-soldered samples (1st reflow cycle), the average shear strength at 100 mm/s is 45.87±3.61 N for conventional joints and 52.14±2.22 N for hybrid joints. At 2000 mm/s, the shear strength of the conventional joints is 52.24±3.63 N, while the hybrid joints demonstrate a higher strength of 64.32±4.18 N. Overall, the shear strength shows minimal variation with increasing reflow cycles for both conventional and hybrid solder joints, with the hybrid joints consistently maintaining higher shear strength than the conventional ones.

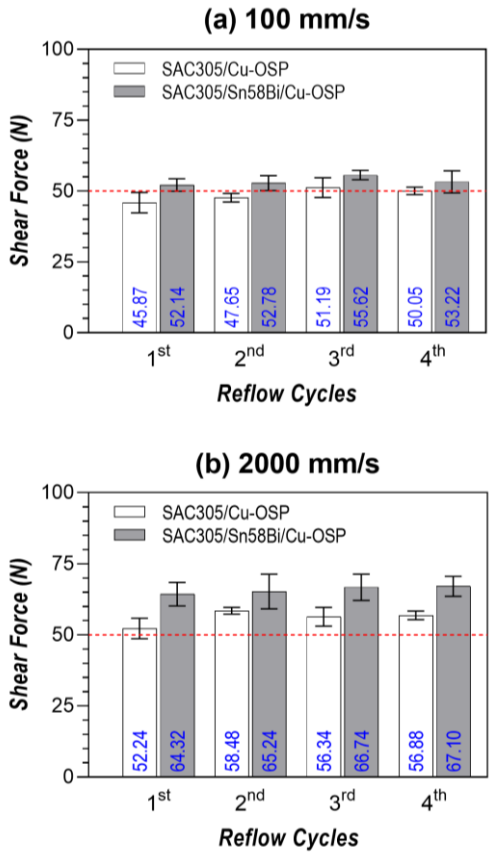

Figure 5. Average shear force as a function of the number of reflow cycles for SAC305/Cu-OSP and SAC305/Sn58Bi/Cu-OSP solder joints, measured at shear speeds of (a) 100 mm/s and (b) 2000 mm/s.

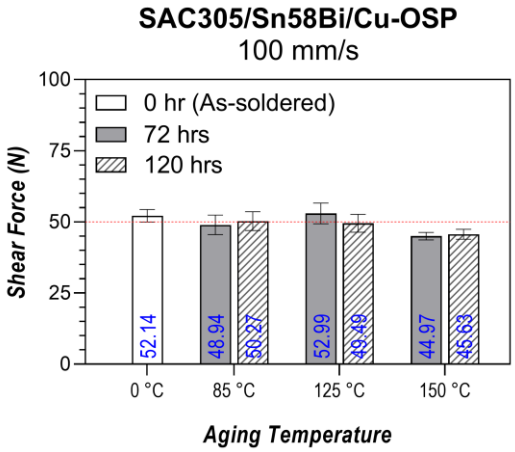

Figure 6. Average shear force of SAC305/Sn58Bi/Cu-OSP hybrid solder joints at 100 mm/s after isothermal aging.

The as-soldered hybrid solder joints were further subjected to isothermal aging at 85 °C, 125 °C, and 150 °C for up to 120 hours to evaluate their reliability. Figure 6 shows the effect of isothermal aging on the shear strength of SAC305/Sn58Bi/Cu-OSP hybrid solder joints at the shear speed of 100 mm/s, particularly in the bulk area.

Overall, the fracture shear force exhibited minimal changes with aging durations of up to 120 hours when aged at 85 °C and 125 °C. However, the shear force was notably lowest when aged at 150 °C, a temperature exceeding the melting point of Sn58Bi at about 138 °C. The hybrid solder joints likely underwent partial remelting and liquid-state aging at this temperature.

These findings highlight the stability of hybrid solder joints under moderate aging conditions, while also identifying potential vulnerabilities at elevated temperatures. Their superior shear strength and thermal performance make them promising candidates for applications that require high mechanical reliability.

4. CONCLUSION

This study assessed the microstructural characteristics and shear strength performance of SAC305/Sn58Bi/Cu-OSP hybrid solder joints under multiple reflow cycles and isothermal aging, comparing them to conventional SAC305/Cu-OSP solder joints. The key findings are summarized as follows:

(i) The SAC305/Sn58Bi/Cu-OSP hybrid solder joints exhibit two distinct microstructural regions: a Bi-rich phase concentrated at the bottom and an Ag-rich phase predominantly distributed throughout the solder bulk at the top.

(ii) Hybrid solder joints exhibited higher shear strength than conventional SAC305/Cu-OSP joints, with 52.14 ± 2.22 N vs. 45.87 ± 3.61 N at 100 mm/s, and 64.32 ± 4.18 N vs. 52.24 ± 3.63 N at 2000 mm/s. The shear strength showed minimal variation with increasing reflow cycles for both joint types, with hybrid joints consistently exhibiting higher strength than conventional ones.

(iii) The fracture shear force showed minimal variation after aging durations of up to 120 hours at 85 °C and 125 °C, indicating good thermal stability. However, at 150 °C, the shear force decreased significantly, likely due to partial remelting of the Sn58Bi alloy.

ACKNOWLEDGMENTS

Sincere appreciation is extended to the Faculty of Chemical Engineering & Technology, UniMAP, for their valuable resources and assistance. We also gratefully acknowledge Nihon Superior Co. Ltd. for their support in providing the equipment necessary for the shear test.

REFERENCES

[1] M. I. I. Ramli, M. A. A. M. Salleh, T. Nishimura, H. Yasuda, N. S. M. Zaimi, and K. Nogita, "Liquid/Solid Interaction of Sn-58Bi/Sn-3.0Ag-0.5Cu Dissimilar Joints during Soldering at Low Temperature by In-Situ Synchrotron Imaging," *JOM*, vol. 74, no. 7, pp. 2760–2769, Jul. 2022, doi: 10.1007/s11837-022-05229-9.

[2] C. Cai, J. Xu, H. Wang, and S. B. Park, "A comparative study of thermal fatigue life of Eutectic Sn-Bi, Hybrid Sn-Bi/SAC and SAC solder alloy BGAs," *Microelectronics Reliability*, vol. 119, p. 114065, Apr. 2021, doi: 10.1016/j.microrel.2021.114065.

[3] S. Zhang, X. Jing, J. Chen, K.-W. Paik, P. He, and S. Zhang, "Preparation, characterization and mechanical properties analysis of SAC305-SnBi-Co hybrid solder joints for package-on-package technology," *Materials Characterization*, vol. 208, p. 113624, Feb. 2024, doi: 10.1016/j.matchar.2024.113624.

[4] S. Zhang *et al.*, "Effect of co on the morphology and mechanical properties of the Sn-3.0Ag-0.5Cu/Sn-58Bi composite solder joints on ENEPIG surface," *Materials Characterization*, vol. 209, p. 113674, Mar. 2024, doi: 10.1016/j.matchar.2024.113674.

[5] Y.-A. Shen, "Cu–Cu joint with great strength using In/Sn–58Bi hybrid soldering at low temperature (90 °C)," *Journal of Materials Research and Technology*, vol. 33, pp. 4473–4480, Nov. 2024, doi: 10.1016/j.jmrt.2024.10.108.

[6] G.-J. Park, D.-M. Jang, J.-W. Jang, J.-S. Jang, J.-Y. Jeong, and Y.-J. Kim, "Comparison of thermal-fatigue lives of conventional and hybrid solder joints: Experiment and FE analysis," *Engineering Failure Analysis*, vol. 157, p. 107907, Mar. 2024, doi: 10.1016/j.engfailanal.2023.107907.

[7] S. Zhang *et al.*, "Investigation of isothermal aged Sn-3Ag-0.5Cu/Sn58Bi-Co hybrid solder joints on ENIG and ENEPIG substrate with various mechanical performances," *Materials Today Communications*, vol. 39, p. 108609, Jun. 2024, doi: 10.1016/j.mtcomm.2024.108609.

[8] S. Zhang *et al.*, "Investigation on electromigration failure behavior of SAC305/SnPb micro-hybrid solder joints for package-on-package techniques: Experiment and simulation," *Materials Letters*, vol. 377, p. 137394, Dec. 2024, doi: 10.1016/j.matlet.2024.137394.

[9] F. Wang, Y. Huang, Z. Zhang, and C. Yan, "Interfacial Reaction and Mechanical Properties of Sn-Bi Solder joints," *Materials*, vol. 10, no. 8, p. 920, Aug. 2017, doi: 10.3390/ma10080920.

[10] W. Zhu, W. Zhang, W. Zhou, and P. Wu, "Improved microstructure and mechanical properties for SnBi solder alloy by addition of Cr powders," *Journal of Alloys and Compounds*, vol. 789, pp. 805–813, Jun. 2019, doi: 10.1016/j.jallcom.2019.03.027.

[11] S. Zhang *et al.*, "Incomplete dissolved behavior and mechanical analysis of SnAgCu-SnBi composite solder structures for high-reliable package-on-package techniques," *Materials Characterization*, vol. 215, p. 114157, Sep. 2024, doi: 10.1016/j.matchar.2024.114157.

[12] W. H. Zhong, Y. C. Chan, M. O. Alam, B. Y. Wu, and J. F. Guan, "Effect of multiple reflow processes on the reliability of ball grid array (BGA) solder joints," *Journal of Alloys and Compounds*, vol. 414, no. 1–2, pp. 123–130, Apr. 2006, doi: 10.1016/j.jallcom.2005.07.047.

[13] P. Roumanille *et al.*, "Evaluation of thermomechanical fatigue lifetime of BGA lead-free solder joints and impact of isothermal aging," *Microelectronics Reliability*, vol. 126, p. 114201, Nov. 2021, doi: 10.1016/j.microrel.2021.114201.

[14] Q. Li, W. Zhao, W. Zhang, W. Chen, and Z. Liu, "Research on thermal fatigue failure mechanism of BGA solder joints based on microstructure evolution," *International Journal of Fatigue*, vol. 167, p. 107356, Feb. 2023, doi: 10.1016/j.ijfatigue.2022.107356.

[15] Y. Cui, J. W. Xian, A. Zois, K. Marquardt, H. Yasuda, and C. M. Gourlay, "Nucleation and growth of Ag_3Sn in Sn-Ag and Sn-Ag-Cu solder alloys," *Acta Materialia*, vol. 249, p. 118831, May 2023, doi: 10.1016/j.actamat.2023.118831.

[16] D. Chen *et al.*, "Precipitation processes and phase interface structure of Ag_3Sn during solidification of SnAg3Cu0.5/Cu solder joint," *Vacuum*, vol. 219, p. 112753, Jan. 2024, doi: 10.1016/j.vacuum.2023.112753.

[17] M. Shang *et al.*, "IMC growth mechanism of Sn58Bi/Cu solder joints and its effect on the coarsening of the Bi phase," *Journal of Materials Research and Technology*, vol. 33, pp. 6307–6318, Nov. 2024, doi: 10.1016/j.jmrt.2024.11.006.

[18] G. Ren and M. N. Collins, "Improved Reliability and Mechanical Performance of Ag Microalloyed Sn58Bi Solder Alloys," *Metals*, vol. 9, no. 4, p. 462, Apr. 2019, doi: 10.3390/met9040462.

[19] J.-W. Kim, Y.-C. Lee, S.-S. Ha, and S.-B. Jung, "Failure behaviors of BGA solder joints under various loading conditions of high-speed shear test," *J Mater Sci: Mater Electron*, vol. 20, no. 1, pp. 17–24, Jan. 2009, doi: 10.1007/s10854-008-9588-2.

[20] H. Tsukamoto, T. Nishimura, S. Suenaga, and K. Nogita, "Shear and tensile impact strength of lead-free solder ball grid arrays placed on Ni (P)/Au surface-finished substrates," *Materials Science and Engineering: B*, vol. 171, no. 1–3, pp. 162–171, Jul. 2010, doi: 10.1016/j.mseb.2010.03.092.

[21] K. Liang, Y. Wang, and Z. He, "Experimental and Statistical Study of the Fracture Mechanism of Sn96.5Ag3Cu0.5 Solder Joints via Ball Shear Test," *Materials*, vol. 15, no. 7, p. 2455, Mar. 2022, doi: 10.3390/ma15072455.

[22] S. Chantaramanee and P. Sungkhaphaitoon, "Influence of bismuth on microstructure, thermal properties, mechanical performance, and interfacial behavior of SAC305-xBi/Cu solder joints," *Transactions of Nonferrous Metals Society of China*, vol. 31, no. 5, pp. 1397–1410, May 2021, doi: 10.1016/S1003-6326(21)65585-1.

[23] J. Yan, B. Wang, J. Zhao, L. Zhao, R. Guo, and J. Sheng, "Improvement of heat aging resistance and tensile strength of SAC305/Cu solder joints by multi-element microalloying," *Intermetallics*, vol. 173, p. 108428, Oct. 2024, doi: 10.1016/j.intermet.2024.108428.

[24] Y. Miao *et al.*, "Effects of Sb on the properties and interfacial evolution of SAC305-2Bi-xSb/Cu solder joints," *Journal of Materials Research and Technology*, vol. 30, pp. 9494–9502, May 2024, doi: 10.1016/j.jmrt.2024.06.023.